FACTA UNIVERSITATIS
Series: **Mechanics, Automatic Control and Robotics** Vol.3, N° 11, 2001, pp. 167 - 178

A NEW PRIMAL-MIXED 3^D FINITE ELEMENT

UDC 515.3

Dubravka Mijuca

Faculty of Mathematics, University of Belgrade, Studentski trg 16, P.0. Box 550
11000 Belgrade, Yugoslavia, e-mail: dmijuca@matf.bg ac.yu

Abstract. *This paper discusses properties of a new HC8/9 finite element in the coordinate independent three-dimensional primal-mixed formulation, where displacements and stresses are a priori continuous. The main goal is to show that this element can be reliably used in the analysis of the regular model problems of arbitrary geometry. That is, this low–order element can be used in analysis of model problems without singularities in their domain, in compressible or nearly incompressible elasticity. In the evaluation of the present scheme, no numerical tune-ups are used, such as reduced integration in the analysis of thin structures. To illustrate the properties of the present finite element, usual low and high tests are provided, regarding its solvability, stability and robustness, as well as several numerical examples.*

Key words: *Finite elements, Full theory, Stress continuity, Reliability*

1. INTRODUCTION

In the recent time, the reliability and efficiency of computational mechanics method are in the very focus of the research interest. The reliability in computational mechanics is a property of the utmost importance and it can be observed in two different stages. Firstly, in the stage of designing, reliable finite element method is one that is solvable, accurate, stable and robust [1]. Secondly, in the stage of exploitation, reliability of the system can be defined as the probability that the structure will adequately perform its intended mission for a specified interval of time when operating under specified environmental conditions [2].

On the other hand, efficiency represents the ability to obtain the accuracy of a prescribed level in a reasonable time and it is an important property particularly from the commercial code end users point of view.

There are large number of miscellaneous methods and techniques in computational mechanics today. However, up to now, there is no known finite element scheme applicable to and reliable in broad range of mechanical problems, even if we stay in linear elasticity domain only.

Received 02 February, 2001

As an example, displacement method, a method with great popularity, derived from the principle of minimum potential energy, behaves well only in the analysis of compressible and not bending dominant problems. However, in 3–dimensional analysis of incompressible materials its finite elements may exhibit volumetric locking. Further, in analysis of thick plates and shells transverse shear or membrane locking, as well as zero energy modes may occur. The consequence is that resulting system of finite element equations is not solvable and/or stable anymore. There are number of classical methods for removing locking effects nowadays, as *assumed strain*, *assumed stress, the Kirchhoff mode concept* or *the discrete shear gap concept*. Still, efficiency or accuracy of these techniques is questionable [3]. In addition, stresses although often most important quantities, have to be determined *a posteriori* by differentiation over each finite element, which entails a loss of accuracy [4] and therefore results with unnaturally discontinuous stress picture along element boundaries.

In the limit mechanical situations [4], a more suitable way is to use mixed finite element methods, where two or more fundamental variables are present in the governing equation. However, the value of any mixed formulation lies in its convergence properties. These properties are governed by the stability consideration [5]. On the other hand, stability of mixed formulations depends on fulfillment of two conditions that are, in general case, in opposition to each other. The interested reader can find more about this topic in [4].

In the present paper, the new three-dimensional primal-mixed finite element scheme, with no case dependent hidden features, where displacement and stress fields are continuous and they are calculated simultaneously in arbitrary coordinate systems, is introduced. The main goal of this paper is to examine the main properties of the present 3^D primal-mixed finite element HC8/9, such as its solvability, robustness, and stability.

The present scheme was established after the careful examination of its the two-dimensional counterpart [6-10], where some general objection [4] to primal-mixed finite element methods are shown to be unfounded.

2. Present Formulation

It has been recently numerically proven in two-dimensional case [6] that primal-mixed finite element formulation, having the displacements and stresses as fundamental variables, has many advantages over a primal finite element formulation, where fundamental unknowns are displacements only. Therefore, the weak form of a mixed problem, associated with Hellinger–Reissner variational principle [4, 11] is used:

$$\text{Find } \{\boldsymbol{u},\boldsymbol{T}\} \in H^1(\Omega)^n \times L_2(\Omega)^{n\times n}_{\text{sym}} \text{ such that } \boldsymbol{u}\Big|_{\partial\Omega_u} = \boldsymbol{w} \text{ and:}$$

$$\int_\Omega (\boldsymbol{AT} : \boldsymbol{S} - \boldsymbol{S} : \nabla\boldsymbol{u} - \nabla\boldsymbol{v} : \boldsymbol{T})d\Omega = -\int_\Omega \boldsymbol{v}\cdot\boldsymbol{f}\ d\Omega - \int_{\partial\Omega_t} \boldsymbol{v}\cdot\boldsymbol{p}d\partial\Omega \tag{1}$$

for all $\{\boldsymbol{v},\boldsymbol{S}\} \in H^1(\Omega)^n \times L_2(\Omega)^{n\times n}_{\text{sym}}$ such that $\boldsymbol{v}\Big|_{\partial\Omega_t} = \boldsymbol{0}$.

In this expression $\boldsymbol{A} = \boldsymbol{K}^{-1}$ is the elastic compliance tensor, while $\boldsymbol{S}$ are the weight functions. Space $L(\Omega)^{n\times n}_{sym}$ is the space of all symmetric tensorfields. Because the displacement spaces are the same as in the classical displacement approach, and the stress space can be discontinuous at the element boundaries, it is a straightforward task to construct the elements of the above type. However, for this kind of stress spaces the first stability condition is not satisfied [4], because of the bilinear form $a(\boldsymbol{T},\boldsymbol{S})$ is not coearcive [4]. It was the main reason why stress base functions are chose n to be [7] from continuous space, i.e. $\boldsymbol{T} \in (H^1)^{n\times n}$, the space of all symmetric tensorfields that have square integrable gradient, for the first stability condition is automatically satisfied. This approach has been successfully used by Mirza and Olson [12] for linear triangles and in [7] for bilinear isoparametric quadrilaterals, and the numerical results indicated high accuracy of a model. The problem of solvability of such configurations has been further elaborated in [6,10] according to Zienkiewicz and Taylor [13]. Further, the introduction of stress constraints as essential boundary conditions is discussed in [7]. The full or partial hierarchic interpolation of stresses one order higher than displacements, in order to attain numerical solvability of the scheme, was considered in [8]. The accuracy and efficiency when solved by direct Gaussian elimination procedure were investigated in [9]. Moreover, the stability of the scheme is examined in [10] by the use of numerical inf–sup test in accordance with [5]. The present paper is the first one considering the primal-mixed formulation in three-dimensional analysis. However, it should be noted that in the present paper stress boundary conditions are not introduced but left for the future investigation.

It has been shown in [7] that present scheme can be decomposed for unknown (variable) and known (prescribed) values of the stresses and displacements denoted by the indices v and p respectively:

$$\begin{bmatrix} \mathbf{A}_{vv} & -\mathbf{D}_{vv} \\ -\mathbf{D}_{vv}{}^T & \mathbf{0} \end{bmatrix}\begin{bmatrix} \mathbf{t}_v \\ \mathbf{u}_v \end{bmatrix} = \begin{bmatrix} -\mathbf{A}_{vp} & \mathbf{D}_{vp} \\ \mathbf{D}_{pv}{}^T & \mathbf{0} \end{bmatrix}\begin{bmatrix} \mathbf{t}_p \\ \mathbf{u}_p \end{bmatrix} - \begin{bmatrix} \mathbf{0} \\ \mathbf{f}_p + \mathbf{p}_p \end{bmatrix}. \tag{2}$$

In these expressions, the nodal stresses $t^{L\,st}$ and displacements u_{Kq} components are consecutively ordered in the column matrices **t** and **u** respectively. The members of the matrices **A** and **D** and of the vectors (column matrices) **f** and **p** (discretized body and surface forces) are respectively:

$$A_{\Lambda uv\Gamma st} = \sum_e \int_{\Omega_i} \Omega^N_\Lambda S_N g^a_{(\Lambda)u} g^b_{(\Lambda)v} \boldsymbol{A}_{abcd}\, g^c_{(\Gamma)s} g^d_{(\Gamma)t} T_L \Omega^L_\Gamma d\Omega \tag{3}$$

$$D^{\Gamma q}_{\Lambda uv} = \sum_e \int_{\Omega_i} \Omega^N_\Lambda S_N U^K_a \Omega^\Gamma_K g^a_{(\Lambda)u}\, g^{(\Gamma)q}_{(\Lambda)v} d\Omega \tag{4}$$

$$f^{\Lambda q} = \sum_e \int_{\Omega_i} g^{(\Lambda)q}_a \Omega^\Lambda_M V^M f^a d\Omega \tag{5}$$

$$p^{\Lambda q} = \sum_e \int_{\partial\Omega_{it}} g^{(\Lambda)q}_a \Omega^\Lambda_M V^M p^a d\partial\Omega \tag{6}$$

3. THE FINITE ELEMENT HC8/9

The present finite element HC8/9 is shown in Fig 1. In the present notation, letter H stands for element hexahedral geometry, while letter C represents continuous interpolation of displacement and stress fields. Displacement nodes at eight corner nodes are denoted by the sphere, while stress nodes are denoted by the tetrahedrons.

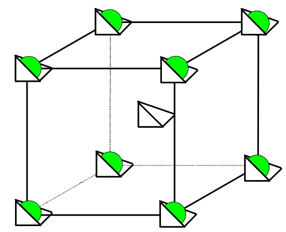

Fig. 1. Finite element HC8/9.

Both fields are approximated by the tri-linear interpolation functions P_1–P_8 given in Equation (7). In addition, stress field is enriched by tri-quadratic hierarchic functions P_9 shown in Equation (8) connected to the central, so-called *bubble* node.

$$\begin{aligned}
&P_1(\xi^1,\xi^2,\xi^3)=\frac{1}{8}(1-\xi^1)(1-\xi^2)(1-\xi^3);\ P_2(\xi^1,\xi^2,\xi^3)=\frac{1}{8}(1+\xi^1)(1-\xi^2)(1-\xi^3)\\
&P_3(\xi^1,\xi^2,\xi^3)=\frac{1}{8}(1+\xi^1)(1+\xi^2)(1-\xi^3);\ P_4(\xi^1,\xi^2,\xi^3)=\frac{1}{8}(1-\xi^1)(1+\xi^2)(1-\xi^3)\\
&P_5(\xi^1,\xi^2,\xi^3)=\frac{1}{8}(1-\xi^1)(1-\xi^2)(1+\xi^3);\ P_6(\xi^1,\xi^2,\xi^3)=\frac{1}{8}(1+\xi^1)(1-\xi^2)(1+\xi^3)\\
&P_7(\xi^1,\xi^2,\xi^3)=\frac{1}{8}(1+\xi^1)(1+\xi^2)(1+\xi^3);\ P_8(\xi^1,\xi^2,\xi^3)=\frac{1}{8}(1-\xi^1)(1+\xi^2)(1+\xi^3)
\end{aligned} \tag{7}$$

$$P_9(\xi^1,\xi^2,\xi^3)=(1-(\xi^1)^2)-(1-(\xi^2)^2)-(1-(\xi^3)^2) \tag{8}$$

Consequently, this element has twenty-four displacement degrees of freedom and fifty-four stress degrees of freedom, which is totally seventy-eight. The numerical integration is performed by 3×3×3 Gausian integration. The subject of the future investigation should be more appropriate, from the point of the stress space finite element test and trial sub-spaces, analysis by 4×4×4 Gausian integration.

Present element has its two-dimensional counterpart QC4/5 that is presented in detail in [6].

4. The low order tests

Some authors consider the following tests as folklore nowadays. However, they are usually, and they should be, first steps in the reliability investigation of any new finite element.

4.1 The compatibility test

The compatibility test demands that displacements are continuous over each element and at the edges of adjacent elements [14]. In the present formulation, the test and trial displacement subspaces are continuous across the interelement boundaries i.e., these belonging to the space $(H^1)^{n\times n}$, so this criterion is satisfied.

4.2 Patch test – necessary solvability conditions

Necessary conditions for the solvability of the Equation (2) can be checked by the patch test of Zienkiewicz and Taylor [13]. Configurations of one or more finite elements, passes patch test if the number of the stress degrees of freedom n_t is greater than the number of displacements degrees of freedom n_u. That is clearly fulfilled in the case of the present finite element HC8/9 (see Section 3.).

4.3. Solvability test - sufficient solvability conditions

One finite element, free of boundary conditions, passes sufficient solvability test [15] if the number of zero eigenvalues of the system matrix in Equation (2) is equal to the number of the rigid body modes. In the three-dimensional case that number is six. If it is greater than six, some mechanisms are present and problem is not solvable. In the present case, the number of the positive eigenvalues corresponds to the number of stress degrees of freedom. While, the total number of zero and negative eigenvalues is equal to the number of displacement degrees of freedom (in this case 8×3=24). This test is performed over the single finite element in the shape of unit square block that is free of boundary conditions. The results in Table 1. show that present HC8/9 finite element passes the solvability test, i.e. the element matrix does not contain *mechanisms*.

Table 1. The primal–mixed finite element HC8/9 solvability test.

The one 3^D primal–mixed finite element HC8/9 system matrix eigenvalue test. The unit square block with E=1 and ν=0.3											
mode	Eigen-value	mode	Eigen-value	mode	Eigen-value	Mode	Eigen-value	mode	Eigen-value	mode	Eigen-value
1	-.2824	14	-.0453	27	.0061	40	.0223	53	.0662	66	.1678
2	-.2500	15	-.0453	28	.0079	41	.0350	54	.0662	67	.1678
3	-.2500	16	-.0367	29	.0079	42	.0350	55	.0689	68	.1678
4	-.2500	17	-.0367	30	.0079	43	.0350	56	.0689	69	.1708
5	-.2079	18	-.0367	31	.0123	44	.0361	57	.0689	70	.1708
6	-.2079	***19***	***.0000***	32	.0123	45	.0361	58	.0772	71	.1708
7	-.1212	***20***	***.0000***	33	.0123	46	.0361	59	.0772	72	.2295
8	-.0928	***21***	***.0000***	34	.0149	47	.0361	60	.0772	73	.3778
9	-.0928	***22***	***.0000***	35	.0179	48	.0361	61	.0952	74	.5195
10	-.0928	***23***	***.0000***	36	.0179	49	.0361	62	.0952	75	.5195
11	-.0856	***24***	***.0000***	37	.0179	50	.0484	63	.0952	76	.8741
12	-.0856	25	.0022	38	.0223	51	.0484	64	.1536	77	.8741
13	-.0856	26	.0061	39	.0223	52	.0662	65	.1536	78	.8741

4.4 The robustness test

To appraise the behavior of the finite element HC8/9 in the nearly incompressible limit an eigenvalue analysis for a single finite element for increasing values of Poisson's ratio [16] was performed. For a volumetric locking-free finite element, only one mode corresponding to the dilatational mode should tend to zero as $\nu \to 1/2$. The single finite element model with 12 suppressed displacement degrees of freedom, shown in Fig 2, was used throughout the test. Results in Table 2 show that finite element HC8/9 can be recommended for the use in compressible or nearly incompressible analysis only, where present system given by Equation (2) is solvable.

Table 2. The primal–mixed finite element HC8/9 robustness test.

The one 3^D primal–mixed finite element HC8/9 system matrix eigenvalue test. The unit square block with E=1.						
ν	Eigenvalues of modes 1 to 66					
0.49	-.1836688	-.1821945	-.1821945	-.1755433	-.1275837	-.1275837
	-.0789815	-.0608021	-.0608021	-.0506589	-.0386173	-.0386173
	.0000932	***.0011561***	.0022732	.0022732	.0030336	.0056919
	.0068981	.0068981	.0137963	.0137963	.0137963	.0206943
	.0206943	.0206943	.0207818	.0207818	.0220340	.0233966
	.0233966	.0413889	.0413889	.0413889	.0413889	.0413889
	.0413889	.0451094	.0503464	.0503464	.0630946	.0639866
	.0639866	.0761568	.0761568	.0828782	.1215745	.1215999
	.1215999	.1376479	.1376479	.1491287	.1491287	.1526186
	.1526186	.1540307	.1780439	.1972095	.2391503	.2399351
	.2399351	.4022241	.4022241	.7658175	.7658278	.7658278
0.499	-.2304078	-.1583840	-.1560167	-.1560167	-.1154086	-.1154086
	-.0787982	-.0607949	-.0607949	-.0505239	-.0385353	-.0385353
	.0000090	***.0000753***	.0009157	.0020524	.0020524	.0069402
	.0069402	.0099848	.0138798	.0138798	.0138798	.0208194
	.0208194	.0208194	.0217715	.0217715	.0221649	.0235292
	.0235292	.0416388	.0416388	.0416388	.0416388	.0416388
	.0416388	.0453723	.0505967	.0505967	.0545396	.0545396
	.0660585	.0684171	.0684171	.0774875	.0774875	.0832877
	.1043810	.1047444	.1047444	.1402004	.1407522	.1407522
	.1497592	.1497592	.1532339	.1532339	.1546110	.1977475
	.2308859	.4756478	.4756478	.8547750	.8547954	.8547954
0.5	-.1833988	-.1818851	-.1818851	-.1767768	-.1273841	-.1273847
	-.0787779	-.0609434	-.0609434	-.0505089	-.0385262	-.0385262
	.0000009	***.0000060***	.0008892	.0020281	.0020281	.0049377
	.0069444	.0069444	.0138888	.0138888	.0138888	.0203116
	.0203116	.0208332	.0208332	.0208332	.0221794	.0235439
	.0235439	.0416666	.0416666	.0416666	.0416666	.0416666
	.0416666	.0454016	.0506245	.0506245	.0635170	.0644135
	.0644135	.0765626	.0765626	.0833333	.1223874	.1224132
	.1224132	.1380419	.1380419	.1498293	.1498293	.1532652
	.1532652	.1546756	.1767768	.1978074	.2397441	.2405394
	.2405394	.4043983	.4043983	.7704236	.7704338	.7704338

5. THE HIGH ORDER TEST – STABILITY

The finite element is stable if it satisfy two necessary conditions i.e., the first condition represented in the *ellipticity on the kernel* condition and second condition represented in the *inf-sup* condition [4].

In the present case, the test and trial stress local functions are from space $(H^1)^{n\times n}$ that ensures that their bilinear form $a: T\times S \rightarrow 0$ is coercive. From that reason, the first condition is automatically satisfied, like in the, for example, Stokes problems [4].

The second condition for stability is satisfied if for the meshes of increasing density, value μ_{min} following from LBB (Ladyzhenskaya, Babuška, Brezzi) condition, remains bounded above zero. This value can be determined as the smallest eigenvalue of the generalized eigenvalue problem as defined in [17], p.76, Eq.(3.22):

$$\mu_{\min} = \inf_{u \in H^1} \sup_{T \in L^2} \frac{b(\boldsymbol{T}_h, \boldsymbol{u}_h)}{\| \boldsymbol{T}_h \| \| \boldsymbol{u}_h \|}, \tag{9}$$

where,

$$b(\boldsymbol{T}_h, \boldsymbol{u}_h) = \sum_e \int_{\Omega_i} \boldsymbol{T}_h : \nabla \boldsymbol{u}_h d\Omega_e \,, \; \| \boldsymbol{T}_h \|^2 = \sum_e \int_{\Omega_i} \boldsymbol{T}_h : \boldsymbol{T}_h d\Omega \,, \; \| \mathbf{u}_h \|^2 = \sum_e \int_{\Omega_i} \nabla \mathbf{u}_h{}^{\mathrm{T}} : \nabla \mathbf{u}_h d\Omega \,. \tag{10}$$

Because verification of condition like (9) involves an infinite number of meshes, a numerical inf-sup test should be performed for a sequence of three or four of meshes, according to of Chapelle and Bathe [5]. Consequently, in the present case, numerical *inf-sup* test in matrix notations is stated as follows:

$$\mathbf{D}^{\mathrm{T}} \mathbf{A}^{-1} \mathbf{D} \, \mathbf{u}_i = \mu_i^2 \mathbf{K} \, \mathbf{u}_i \,, \tag{11}$$

where **D** and **A** are matrix entries in (2), while matrix **K** is the stiffness matrix from the relating primal i.e. displacement method (see [6] for details). This approach is already use in [6] where the stability of primal-mixed Taylor-Hood type two-dimensional finite element in elasticity was firstly proven.

Throughout the test the simple unit square block, shown in Fig. 2, is used. The obtained results given in Fig. 3. and Table 3, show that finite element HC8/9 has $\mu^2_{\min}$= {1;0.6917;04746} in one, eight and twenty seven element model problems respectively, so evidently - it is not stable. It is worthy to note that its two-dimensional counterpart QC4/5 fails this test also, although it is very effective for regular problems [6].

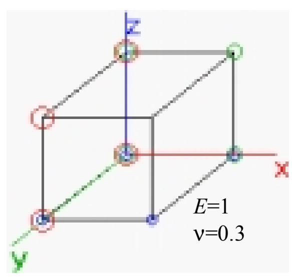

Fig. 2. The inf-sup test model problem.

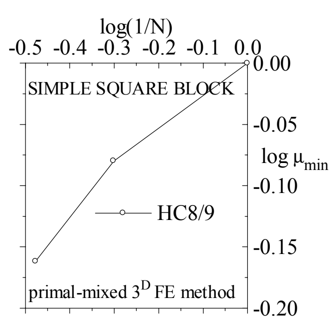

Fig. 3. Inf-sup results.

Table 3. Inf sup results.

	Inf-sup test of 3^D finite element HC8/9									
No. of elements	Eigenvalues μ_i of generalized eigenvalue problem given by Eq. (11)									
1×1×1 =1	***1.0000***	1.0000	1.0000	1.0000	1.0000	1.0000	1.0000	1.0000	1.0000	1.0000
	1.0000	1.0000								
2×2×2 =8	0.9088	0.8925	0.8881	0.8687	***0.6917***	0.7935	0.8296	0.8206	0.8836	0.8836
	0.8789	0.8789	0.8594	0.8594	0.6973	0.6973	0.6973	0.7127	0.7127	0.8333
	0.8333	0.7384	0.8097	0.8097	0.8136	0.8136	0.8111	0.7583	0.7264	0.7308
	0.7308	0.7618	0.7618	0.7422	0.7422	0.7443	0.7455	0.7455	0.7543	0.7543
	0.7565	0.7565	1.0000	1.0000	1.0000	1.0000	1.0000	1.0000	1.0000	1.0000
	1.0000	1.0000	1.0000	1.0000						
3×3×3 =27	0.4848	0.4747	0.4997	***0.4776***	0.4776	0.4859	0.4889	0.4889	0.4929	0.5063
	0.5063	0.5370	0.5441	0.5148	0.5148	0.5157	0.5173	0.5307	0.5307	0.5571
	0.5581	0.5350	0.5820	0.5498	0.5590	0.5590	0.6054	0.6035	0.6054	0.6337
	0.6174	0.6174	0.6383	0.6226	0.6226	0.9762	0.9708	0.6356	0.6356	0.6590
	0.6507	0.9616	0.6468	0.6508	0.6508	0.6616	0.6803	0.6673	0.8170	0.6848
	0.6721	0.6763	0.6763	0.7968	0.7278	0.7319	0.7027	0.6955	0.6856	0.6856
	0.7154	0.7475	0.7599	0.7807	0.6948	0.6954	0.6954	0.7016	0.7067	0.7067
	0.7096	0.7145	0.7172	0.7172	0.7377	0.7424	0.7571	0.7528	0.7528	0.7542
	0.7542	0.7876	0.7876	0.7779	0.7779	0.9544	0.9759	0.9759	0.9478	0.9665
	0.8344	0.8540	0.8496	0.8453	0.8453	0.9320	0.9413	0.9413	0.9254	0.8500
	0.8500	0.8754	0.8607	0.9324	0.9324	0.9294	0.9178	0.9105	0.8813	0.8949
	0.8717	0.8698	0.8698	0.9029	0.9187	0.9187	0.9119	0.9155	0.9155	0.8936
	0.8936	0.8888	0.8888	0.8857	0.8830	0.8831	0.8831	0.9007	0.9007	0.9036
	0.9041	0.9041	1.0000	1.0000	1.0000	1.0000	1.0000	1.0000	1.0000	1.0000
	1.0000	1.0000	1.0000	1.0000						

6. Numerical Examples

The performance of the 3D finite element HC8/9 is evaluated by considering standard examples. Isotropic, homogeneous material property and linear elasticity behaviour are assumed.

6.1 Pure shear of a thin plate.

A problem of a thin rectangular plate of dimensions 1×0.01×1 subjected to a pure shear is considered. Modulus of elasticity is E=1·10^{11} and Poisson's ratio is ν=0.3. The finite element model consisting of one element and its scaled deformed configuration, are shown in Fig. 4. The some of input values and *exact* solution of a problem, are given in Table 3.

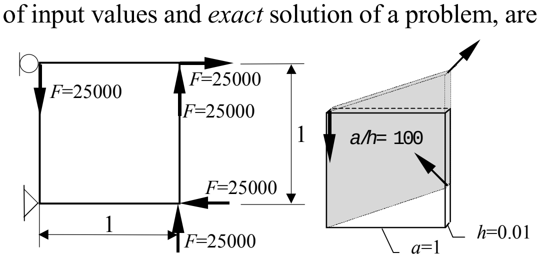

Fig. 4. The pure shear of a thin plate.

Displacement and stress results reported in Tables 4 and 5, respectively, point out that present finite element HC8/9 has excellent performance.

Table 3. The pure shear of a thin rectangular plate 1×0.01×1, E=1·10^{11} ,ν=0.3.

Node	Input values									Exact solution		
	Model geometry			boundary conditions: 1 – free, 0 – zero			Input forces			u_z	t^{xz}	u_x,u_y t^{xx},t^{yy}, t^{zz},t^{xy},t^{yz}
	x	y	z	bc u	bc v	bc z	F_x	F_y	F_z			
1	0	0	0	0	0	0	0.	0.	0.	0.	1E+7	0.
2	1	0	0	1	0	1	-25000	0.	25000	.26E-03	1E+7	0.
3	1	0.01	0	1	0	1	-25000	0.	25000	.26E-03	1E+7	0.
4	0	0.01	0	0	0	0	0.	0.	0.	0.	1E+7	0.
5	0	0	1	0	0	1	0.	0.	-25000	0.	1E+7	0.
6	1	0	1	1	0	1	25000	0.	25000	.26E-03	1E+7	0.
7	1	0.01	1	1	0	1	25000	0.	25000	.26E-03	1E+7	0.
8	0	0.01	1	0	0	1	0.	0.	-25000	0.	1E+7	0.

Table 4. Displacement solution obtained with HC8/9 finite element.

Displacements in the pure shear of a thin rectangular plate.			
Node	u_x	u_y	u_z
1	.0000E+00	.0000E+00	.0000E+00
2	.1455E-15	.0000E+00	.2600E-03
3	.1455E-15	.0000E+00	.2600E-03
4	.0000E+00	.0000E+00	.0000E+00
5	.0000E+00	.0000E+00	-.2157E-16
6	-.1335E-15	.0000E+00	.2600E-03
7	-.1335E-15	.0000E+00	.2600E-03
8	.0000E+00	.0000E+00	-.2157E-16

Table 5. Stress solution obtained with HC8/9 finite element.

Stress state in the pure shear of a thin rectangular plate.						
Node	t^{xx}	t^{yy}	t^{zz}	t^{xy}	t^{xz}	t^{yz}
1	18348E-04	.71546E-05	.54998E-05	-.47476E-11	.1000E+08	-.68947E-07
2	.19217E-04	.80222E-05	.75244E-05	.13066E-09	.1000E+08	-.14356E-06
3	.19223E-04	.80297E-05	.75416E-05	.52745E-11	.1000E+08	.26057E-06
4	.18346E-04	.71504E-05	.54905E-05	.96886E-11	.1000E+08	-.92243E-07
5	-.19222E-04	-.89494E-05	-.10609E-04	.32957E-10	.1000E+08	.56677E-07
6	-.18354E-04	-.80819E-05	-.85852E-05	-.15903E-09	.1000E+08	-.59987E-07
7	-.18334E-04	-.80617E-05	-.85379E-05	.45325E-10	.1000E+08	-.25696E-06
8	-.19225E-04	-.89532E-05	-.10618E-04	-.76076E-10	.1000E+08	.19047E-06

6.2 Hydrostatic pressure in incompressible materials.

To assess the performance of the present three-dimensional finite element HC8/9 in nearly incompressible and incompressible state, a problem of the unit square block subjected to a hydrostatic pressure p=1, is considered. The elastic modulus was taken as E=0.02·10^8 (rubber), while Poisson's ratio was gradually increased. The model problem is discretized by one finite element.

The displacement and stress results for different values of Poisson's ratio are given in Table 6. Present finite element HC8/9 shows excellent performance in the nearly incompressible state, while results slightly deteriorate for Poisson's value greater than ν=0.4999999999.

Table 6. The behavior of 3^D finite element HC8/9 toward incompressibility.

The unit square block model problem, $E=0.02\cdot 10^8$

$\nu=0.4999999$									
Node	u_x	u_y	u_z	t^{xx}	t^{yy}	t^{zz}	t^{xy}	t^{xz}	t^{yz}
1	.00E+00	.00E+00	.00E+00	.10E+01	.10E+01	.10E+01	.54E-22	-.31E-22	.19E-22
2	.10E-12	.00E+00	.00E+00	.10E+01	.10E+01	.10E+01	.23E-15	.21E-15	-.46E-22
3	.10E-12	.10E-12	.00E+00	.10E+01	.10E+01	.10E+01	.33E-15	-.18E-15	-.21E-16
4	.00E+00	.10E-12	.00E+00	.10E+01	.10E+01	.10E+01	.95E-16	-.33E-22	.98E-16
5	.00E+00	.00E+00	.10E-12	.10E+01	.10E+01	.10E+01	-.16E-22	.11E-15	.17E-15
6	.10E-12	.00E+00	.10E-12	.10E+01	.10E+01	.10E+01	-.16E-15	.33E-15	-.20E-15
7	.10E-12	.10E-12	.10E-12	.10E+01	.10E+01	.10E+01	-.19E-15	-.45E-15	-.22E-15
8	.00E+00	.10E-12	.10E-12	.10E+01	.10E+01	.10E+01	-.24E-16	-.26E-15	.27E-15
$\nu=0.4999999999$									
Node	u_x	u_y	u_z	t^{xx}	t^{yy}	t^{zz}	t^{xy}	t^{xz}	t^{yz}
1	.00E+00	.00E+00	.00E+00	.10E+01	.10E+01	.10E+01	-.10E-24	.72E-25	.25E-25
2	.10E-15	.00E+00	.00E+00	.10E+01	.10E+01	.10E+01	.91E-16	.15E-15	-.90E-25
3	.10E-15	.10E-15	.00E+00	.10E+01	.10E+01	.10E+01	.75E-16	-.19E-15	.17E-15
4	.00E+00	.10E-15	.00E+00	.10E+01	.10E+01	.10E+01	-.15E-16	-.45E-25	-.21E-16
5	.00E+00	.00E+00	.10E-15	.10E+01	.10E+01	.10E+01	.81E-25	-.12E-15	-.20E-15
6	.10E-15	.00E+00	.10E-15	.10E+01	.10E+01	.10E+01	-.25E-15	.25E-16	.60E-16
7	.10E-15	.10E-15	.10E-15	.10E+01	.10E+01	.10E+01	-.81E-16	-.61E-16	.23E-15
8	.00E+00	.10E-15	.10E-15	.10E+01	.10E+01	.10E+01	.17E-15	.13E-15	-.22E-15
$\nu=0.5$									
Node	u_x	u_y	u_z	t^{xx}	t^{yy}	t^{zz}	t^{xy}	t^{xz}	t^{yz}
1	.00E+00	.00E+00	.00E+00	.54E+00	.54E+00	.54E+00	-.33E-30	-.49E-30	.98E-31
2	-.23E-21	.00E+00	.00E+00	.56E+00	.56E+00	.56E+00	-.23E-15	-.96E-16	-.49E-31
3	-.59E-21	.59E-22	.00E+00	.54E+00	.54E+00	.54E+00	-.41E-15	-.89E-16	-.35E-16
4	.00E+00	.326E-21	.00E+00	.56E+00	.56E+00	.56E+00	-.17E-15	.22E-30	.15E-15
5	.00E+00	.00E+00	-.11E-20	.56E+00	.56E+00	.56E+00	.50E-30	.33E-15	.35E-15
6	-.38E-21	.00E+00	-.60E-21	.54E+00	.54E+00	.54E+00	-.23E-15	.24E-15	.18E-15
7	-.72E-21	.536E-23	-.33E-21	.56E+00	.56E+00	.56E+00	-.60E-15	.73E-16	.14E-15
8	.00E+00	.56E-21	-.57E-21	.54E+00	.54E+00	.54E+00	-.37E-15	.16E-15	.51E-15

6.3 Thin clamped twisted beam.

This is one of most severe benchmark test for testing the effect of warping on the behavior of finite elements [18, 19]. The twisted beam plate is of dimensions 12×1.1×0.05 and it is subjected to in–plane and out of plane tip concentrated loads F=1N. Modulus of elasticity is $E=2.9\cdot 10^7$ and Poisson's ratio is $\nu=0.22$. The beam is clamped at one end and twisted by 90^0 on its free end.

Displacement results obtained by present finite element HC8/9, for both load cases, as well as theoretical results of interest [18], are given in Table 7. It is interesting to note that deformation v from out of plane loading is same as deformation u from in-plane loading.

The undeformed and deformed configurations for out of plane loading of model 12×4×2, in x-y view, are visualized in Fig. 5. The visualisation of the dominant stress component for the same model problem is given in Fig. 6.

Table 7. Deflection of nodes obtained by HC8/9 finite elements.

Thin twisted beam						
	Out of plane loading F={-1,0,0}.			– In-plane loading F={0,-1,0}.		
model	u	v	w	u	v	w
12×1×1	-.1360315	-.1848626	.138635E-01	-.1848654	-.3192102	.796448E-03
12×2×2	-.1406048	-.1911060	-.299778E-12	-.1911060	-.3284138	-.243203E-01
12×4×2	-.1416732	-.1925537	-.162740E-11	-.1925537	-.3305027	.244896E-01
24×4×2	-.3070082	-.4334642	.162479E-11	-.4334642	-.9536279	.395472E-11
48×4×2	-.3314389	-.4741882	-.671485E-08	-.4741882	-1.249587	-.641611E-08
theory [18]	*-.343100*				*-1.390000*	

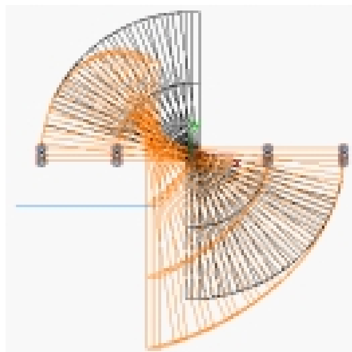

Fig. 5. The thin twisted beam model 12×4×2 – view *xCy*.

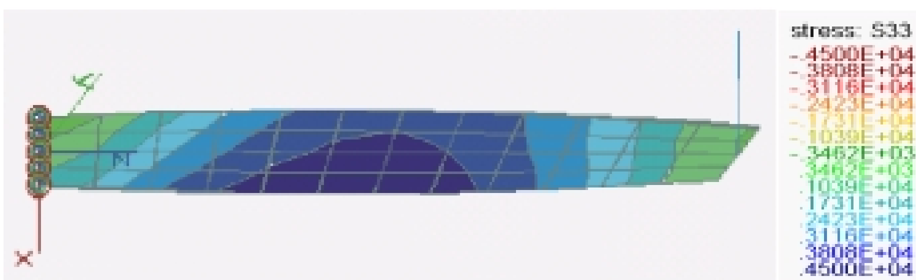

Fig. 6. The thin twisted beam model 12×4×2 – dominant stress t^{11}component.

CONCLUSION

The preliminary investigation of a new full three-dimensional primal-mixed finite element method, that allows simultaneous continuous approximation of stress and displacement fields, employing low order finite element HC8/9, is presented. The present finite element exhibits a good behavior without experiencing any locking phenomena or *zero* energy modes, performing well for compressible and nearly incompressible materials, regardless of model problem geometrical characteristics.

REFERENCES

1. Bathe K.J. *On reliability in the simulation of structural and fluid flow response.* Advances in computational methods for simulation, Civil-Comp Press, Edinburgh, 1–7, 1996.
2. Noor A.K. *Computational structures technology - leap frogging into the twenty-first century.* Advances in Computational Structures Technology, Civil-Comp Press, 1–18, 1996.
3. Wall W.A., Gee M. and Ramm E., *The challenge of a three–dimensional shell formulation – the conditioning problem*, Fourth International Colloquium on Computation of Shell & Spatial Structures, Chania-Crete, Greece, 2000.
4. Arnold D.N., *Mixed finite element methods for elliptic problems*, Computer Methods in Applied Mechanics and Engineering, 1990, **82**, 281-300.
5. Chapelle D. and Bathe K.J., *The inf-sup test, Computers & Structures*, 1993, **47**, No. 4/5, 537–545.
6. Mijuca D. *Primal-mixed finite element approach in solid mechanics*, Ph.D. Thesis, Faculty of Mathematics, Belgrade (in Serbian), 1999.
7. Berković M. and Drašković Z., *A two-field finite element model related to the Reissner's principle*, Theoretical and Applied Mechanics, 1994, **20**, 17-36.
8. Berković M., Drašković Z. and Mijuca D., *A direct block sparse solution of the mixed finite element equations*, Compt. Assisted Mechanics and Engineering Sciences, 1998, **5**, 21–30.
9. Mijuca D. and Berković M., *On the efficiency of the primal-mixed finite element scheme*, Advances in Computational Structured Mechanics, Civil-Comp Press, 1998, 61–69.
10. Berković M. and Mijuca D., *On the main properties of the primal-mixed finite element formulation*, Facta Universitatis Series Mechanics, Automatic Control And Robotics, Vol, 2, No 9, 903–920 1999.
11. Wempner G., *Mechanics of solids with applications to thin bodies*, McGraw–Hill, 1973.
12. Mirza F.A. and Olson M.D., *The mixed finite element in plane elasticity*, International Journal of Numerical Methods in Engineering, 1980, Vol 15, 273–289.
13. Zienkiewicz O.C. and Taylor R.L., [1989], *The Finite Element Method* VOL I, McGraw–Hill, London.
14. Bathe K.J., *Finite element procedure*, Prentice Hall, 1982.
15. Olson M.D., *The mixed finite element method in elasticity and elastic contact problems*, in S.N. Atluri, R.H.Gallagher and O.C.Zienkiewicz, eds. *Hybrid and Mixed Finite Element Methods*, John Wiley & Sons, 19–49, 1983.
16. Kasper E.P. and Taylor R.L., *A mixed-Enhanced Strain Method: Linear Problems*, University of California, Report No.UCB/SEMM-97/02, 1997.
17. Brezzi F.and Fortin M., *Mixed and Hybrid Finite Element Methods*, Springer-Verlag, New York, 1991.
18. Simo J.C. and FOX D.D., *On a stress resultant geometrically exact shell model*. Part II. The linear theory, computational aspects. Comput. Methods Appl. Mech. Engrg, Vol 73, 53-92, 1989.
19. Kojić M, Slavković R., Živković M., Grujović N., *Finite element method I* (in Serbian), Faculty of Mechanical Engineering, Kragujevac, 1998.

NOVI TRODIMENZIONI KONAČNI ELEMENT

Dubravka Mijuca

U radu se predstavlja novi trodimenzioni konačni element za pouzdanu analizu linearno-elastičnih kompresibilnih i skoro inkompresibilnih tela proizvoljnih geometrijskih karakteristika, a pod proizvoljnim opterećenjima. Dati element je razvijen nad prostorima probnih i test funkcija najnižeg reda, a za koje je polazna primalno-mešovita formulacija rešiva. Rešivost, robustnost i stabilnost posmatranog konačnog elementa HC8/9 ispitivana je uobičajenim testovima